RSC Advances

Microbial cell lysis and nucleic acid extraction via nanofluidic channel

Journal:	*RSC Advances*
Manuscript ID:	RA-ART-01-2015-001336
Article Type:	Paper
Date Submitted by the Author:	26-Jan-2015

Complete List of Authors:	Kant, Krishna; Flinders University, School of Chemical and Physical Sciences Yoo, Jeongha; The University of Adelaide, School of Chemical Engineering Amos, Steven; The University of Adelaide, School of Chemical Engineering Erkelens, Mason; The University of Adelaide, School of Chemical Engineering Priest, Craig; University of South Australia, Ian Wark Research Institute Shapter, Joe; Flinders University, School of Chemical and Physical Sciences Losic, Dusan; The University of Adelaide, School of Chemical Engineering

RSC Advance

RSCPublishing

ARTICLE

Microbial cell lysis and nucleic acid extraction via nanofluidic channel

Cite this: DOI: 10.1039/x0xx00000x

K. Kant,[a] J. Yoo,[b] S. Amos,[b] M. Erkelens,[b] C. Priest,[c] J.G. Shapter,[a] and D. Losic[*b]

Received 00th January 2012,
Accepted 00th January 2012

DOI: 10.1039/x0xx00000x

www.rsc.org/

This paper presents a microfluidic device with a nano-channel prepared by focused ion beam (FIB) milling for microbial cell lysis and nucleic acid extraction. The device prepared in quartz slide combines two microchannels connected with one nanochannel in the middle with dimensions of 100 nm (width) and 250 nm (depth) and 1µm (length). The capturing of single or few cells and their lysis for extraction of DNA in nanochannel were demonstrated. The purity and quantity of the extracted genetic material was tested using a UV spectrometer. The results revealed that the extraction methodology was successful and may be well-suited to integration in analytical lab-on-a-chip devices.

Introduction

Nanofluidic techniques enable extreme miniaturization of devices and enhanced analytical performance. These devices offer high sensitivity and reproducibility, low consumption of expensive, rare, or hazardous chemicals, and less energy on a single integrated device.[1]

Coupled with advanced analytical techniques, they offer potential in applications from point of care to single cell analysis,[1,2] and other examples where resources are limited.[3,4] It was shown that incorporation of biological membranes and synthetic nanochannels in a device can create new opportunities for advanced analytical applications[5,6] due to the increased surface area and reduced use of chemical reagents.[7,8] Nanofluidic devices may also manipulate cell entities such as proteins, nucleic acids and cell organelles providing ultra-high sensitive analysis using ion source and electrochemical detection.[9] Single-cell analysis can be achieved by integration of several biochemical steps into a micro total analysis system (µTAS) on a single chip.[10,11] However, it is difficult to handle and manipulate single cells in microsystems, since very small volumes are involved in the analysis.[12] The genome of any simple organism may contain thousands of base pairs and it is even more complex in higher species.[13,14] Consequently, an integrated nanofluidic chip is a required approach to handling these tiny volumes of complex cell material without damage or loss. Ideally, all steps from cell lysis to analysis of the molecular cell contents, including DNA analysis, are needed on a single integrated chip.[15-17] Furthermore, integration of several devices for parallel analysis for different molecules is an attractive prospect.

A number of sophisticated fabrication tools have been used to fabricate nanochannels in recent years.[18] E-beam lithography followed by etching has been used to prepare nanochannels (and nanostructures within nanochannels[19]) with certain limitations of length and depth (depends on reactive ion etching (RIE) techniques). Nanoimprint lithography is capable of producing nanofluidic channels with dimensions of 10 nm in width.[11,13,20,21]

In this study, we first introduce the potential of cell lysis and extraction of nucleic acids in the nanofluidic device by trapping, lysing, and extracting microbial cells before eluting the genetic material. Moreover, we describe a suitable technique for the fabrication of nanochannels using focused ion beam (FIB) milling. The prepared devices offer an integrated micro- and nanofluidic system, with features that enable several functions performed during chemical analysis (sample preparation, fluid handling and injection, separation, and detection) and new potential for the development of advanced analytical chips.[22,23]

The schematic of the nanofluidic device is presented in Fig. 1. This scheme shows the flow of algae cells used as a model into the microchannels and diffusion of NaCl through the nanochannel for cell lysis. The collected raw material from cell lysis is analyzed using UV/VIS spectrophotometer.

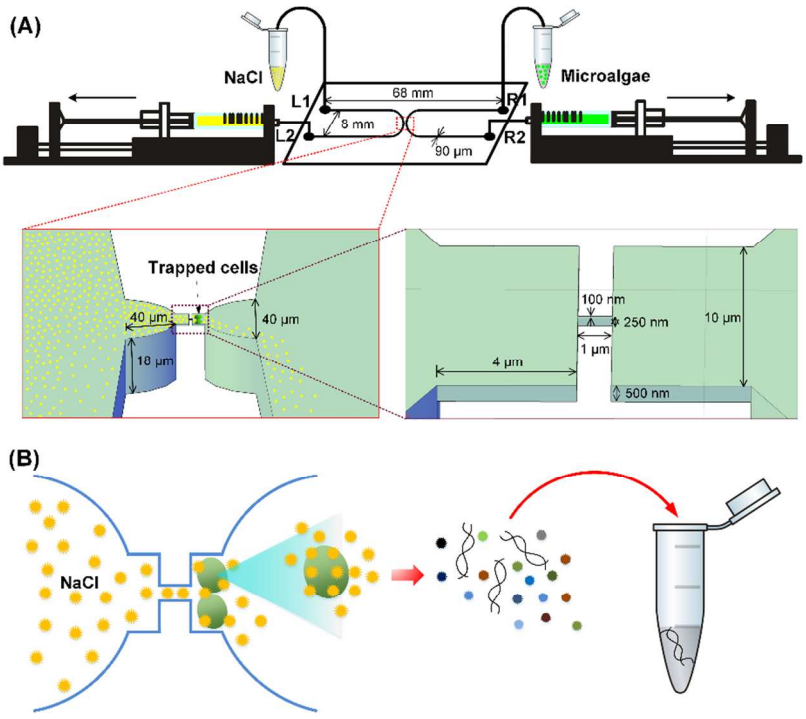

Fig. 1 Schematic of design (A) and concept (B) of a nanofluidic device.

Experimental

Fabrication of microchannel and nanochannel

Microchannels were fabricated by using photolithography and wet chemical etching (Fig. 2(i)). Microfluidic chips were prepared in Quartz (Viosil, from Shin Etsu, Japan). It was first spin-coated with AZ 1518 photoresist (Delta 80, from SUSS MicroTec) and then baked for 1 min at 105°C, the UV exposure was carried out at 340 nm by (EVG 620) Mask Aligner at 120 mJ cm^{-2}. The exposed chip was developed using MIF 726 (Micro-chemicals). After patterning using photolithography, the wet chemical etching of the pattern was then achieved using hydrofluoric acid (HF) for 12 min to achieve 18 µm depth of the micro-channel. After that, photoresist was removed by commercial AZ remover.

The nanochannel was patterned by FIB milling using a Helios NanoLab 600 Dual Beam instrument (FEI Company) as schematically presented in Fig. 2(ii)-(iv). After photolithography the chip was sputtered with 40 nm thick Cr layer to have good controls such as preventing from milling progressively deeper and protecting redeposition of material and structural deformations over the ion beam milling and imaging of channel.[20] The ion beam energy for milling nanostructure is typically between 10 and 50 keV, with beam currents varying between 1 pA and 10 nA.[24] 100 nm width and 250 nm depth nanochannel was milled into a quartz substrate through a 40 nm thick Cr film using an ion beam probe with a beam current of 0.17 nA for 20 keV Ga^+ ions at normal incidence on milling pattern of 100 nm width and 500 nm depth. Before milling the nanochannel to connect the two microchannels an extension in Fig 2(iii) of 10 µm was milled to control the distance between the two big microchannels and provide a flat and smooth surface for final milling of nanochannel. The milled nanochannel in Fig. 2(iv) has Gaussian-like beam profile in the cross sections. Operating in this mode, the width of the nanochannel obtained for a given film thickness and ion beam current is highly reproducible. It is controlled by the user-defined width of the scan area. After milling, Cr was removed using ceric ammonium nitrate.

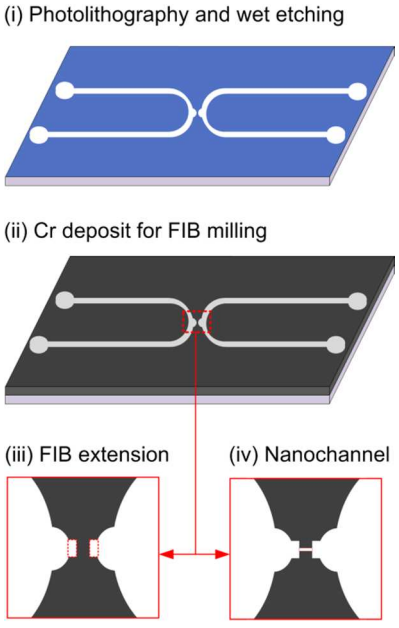

Fig. 2 fabrication of microfluidic chip with nanochannel. (i) Fabrication of microchannel by photolithography and wet etching, (ii) Cr deposition for FIB milling, (iii) Extension of microchannel using FIB milling, and (iv) making a nanochannel in between extended micro-channels.

The access ports were drilled using abrasive powder blasting. The substrate and cover plate are cleaned using piranha solution, their surfaces are activated in an oxygen plasma (Harrick Plasma, 18 W, 10 min), and then they are brought into contact, forming a reversible bond. The bonding is made permanent by heating the device to 1100° in a vacuum furnace and holding at this temperature for >10 h.

Cell injection and lysis into microfluidic channel

Chlorella vulgaris (ATCC30821) was obtained from the American Type Culture Collection (ATCC). It was grown at 25°C with the cap loosened one half turn and maintained under a 14/10 h light-dark photoperiod and subcultured every 14~21 days. To quantify the *C. vulgaris* number, we measured the number of cells using a hemocytomer.

The processes for cell injection, trapping, lysis, and elution in microchip were shown in Fig. 3 in brief. 1×10^5 cells/ml diluted with sterilized in Fig. 3(i) was injected into the R1 port of the microfluidic channel by using a syringe pump (Chemyx, Fusion-200) with flow rate of 3 µl min^{-1}. Once the cells were flowing inside the microfluidic channel, 100 mM NaCl solution for osmotic stresses was injected and maintained with flow rate of 5 µl min^{-1} into the L1 port of the microchannel. In Fig. 3(ii), microalgae cells were trapped in the middle-extended part of the microchannel by changing the flow direction such as from R1 to R2 and from R2 to R1. By changing the direction from L1 to R2 for the flow of NaCl solution, it was flowed across the nanochannel and reached to the other side of the microchannel where the cells were trapped. As soon as the NaCl reached to the other microchannel through the nanochannel, the cell lysis was performed for 30 sec and shown in Fig. 3(iii). After lysis, L1-L2 microchannel was washed by sterilized water with 5 µl min^{-1} flow rate. Then genetic materials of lysed alga cell were eluted by starting flow from R2 to L1 with 2 µl min^{-1} in Fig. 3(iv) and collected in an eppendorf tube.

Instrument analysis

The microfluidic chip was positioned on an fluorescence microscopy (BH 2-UMA, Olympus) to allow monitoring and image data acquisition of the detection of *C. vulgaris* images using Motic Images plus 2.0 software were taken by Moticam 2000 charge-coupled device (CCD) camera inside the microchannel. The cell movement and lysis was observed using a CCD camera at frame rate of 25 frames per second. The change of the fluorescence intensity of the cell after lysis was observed at fluorescence microscope by adopting a 460-490 nm excitation filter and a 515-550 nm emission filter with a mercury lamp.

To determine the quantity and quality of the DNA extracted by the chip, UV/VIS spectrophotometer (Nanodrop, Thermo scientific, DE, USA) was used as a validation method. The quantity of DNA was displayed and purities of nucleic acids were monitored by 260nm/280nm absorbance ratio, which also gives the quality of the DNA extraction.[25]

Result and Discussion

The functionality of the nanofluidic device was initially tested using dye solution. Once flow was demonstrated, indicating that the nanocahnnel fabrication was successful, cell trapping, lysis, and extraction of genetic material were carried out, as described in the following sections.

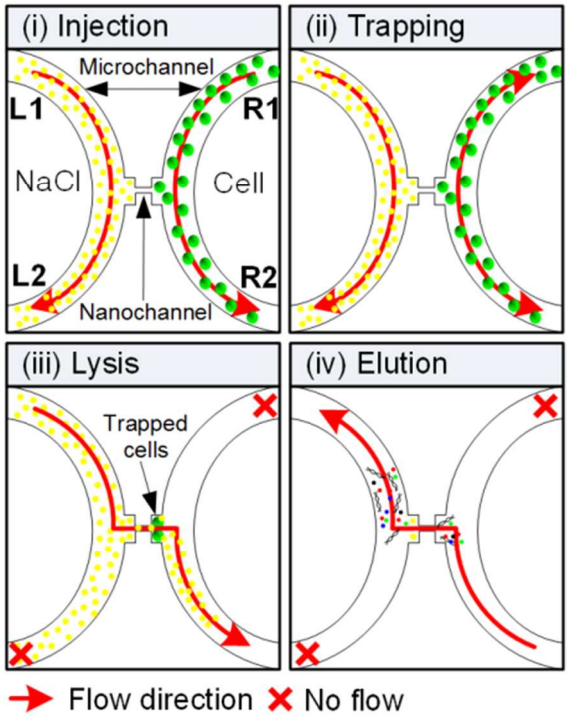

Fig. 3 Schematic representation of microbial cell lysis and nucleic acid extraction using microfludic chip integrated with nanochannel. (i) Alga cells and NaCl are transported in micro-channel and (ii) alga cells were trapped in to the small area (beak) of the microchannel (iii) cell lysis, and then (iv) DNA flows across the nanochannel and collected in to collection vial.

Nanochannel characterization

The SEM images of the fabricated microfluidic channel were taken before and after the FIB milling. In Fig. 4A two microchannels are shown before FIB milling. The distance between the two microchannels was approximately 18 µm depending on the etching time using HF. In this way, the length of the separation between the micro-channels can be controlled. In our case, we used FIB to extend the microchannel segments to adjust the length of the nanochannel and prepare a flat surface for FIB milling of the nanochannel (Fig. 4B). Once we have the extended microchannel using FIB, the distance between the microchannels is much smaller and we can easily mill a nanochannel with low energy (0.17 nA) ion beam in a very short time (2-3 min depending on the Cr layer thickness). The magnified view of the microchannel from Fig. 4B shows the milled extension of the microchannel in Fig. 4C and the image of cross section for a Gaussian-shaped nanochannel with dimensions of 100 nm width, 250 nm depth, and length of 1 µm shows in Fig. 4D. The length of nanochannel can be varied from few hundred nanometer to 20 µm. The width and depth of the fabricated nanochannel is dependent on the input parameters of the pattern and ion beam energy. A small variation in parameter can vary the dimension of the nanochannel; however it is also difficult to control the ion beam from shifting due to the charging effect from the sample surface. However use of low energy beam and recoating on the surface reduces this effect.

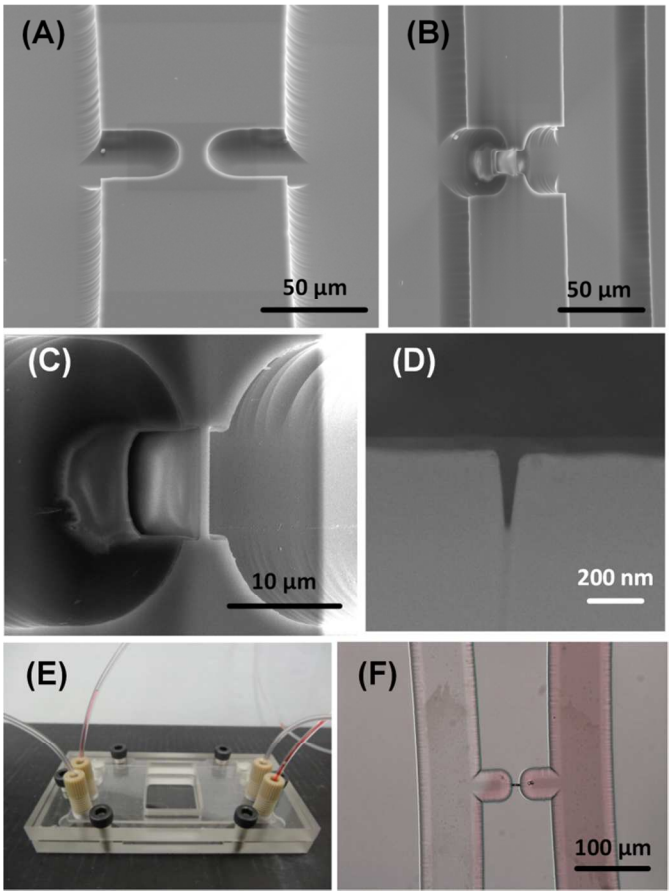

Fig. 4 SEM images of the fabricated micro and nano channels. (A) microchannels after lithography (B) extension of microchannel by FIB milling to achieve required length of nano channel (C) magnified image of the microchannel and nanochannel (D) optical image of actual working device (E) red dye testing to confirm flow through nanochannel (F).

After making the nanochannel on the chip it was cleaned by use of Cr etchant (ceric ammonium nitrate) and bonded under vacuum at 1100℃. This quartz nanochannel chip was then used in the specially designed plastic holder with the inlet and outlet micro bore tubing (Fig. 4E). To confirm that nanochannel was working well and the chip was bonded perfectly we performed a small test with the flow of dye (red fruit dye) in the nano channel. In one microchannel red dye was flowed rate of 10 µl min^{-1} using a syringe pump and the other channel was filled with deionized (DI) water at same rate of flow. Once completely filled with the aqueous dye solution and DI water, the dye solution was pumped through the nanochannels and, after some time, the dye was observed at the left microchannel because the dye diffused by the concentration gradient via nanochannel in Fig. 4F. This demonstrated that the nanochannel was unblocked and able to transport liquid between the channels.

Cell flow and lysis

The algal cells were injected into the right microchannel (R1-R2) with a flow rate of 3 µl min^{-1}. Once the microchannel was filled with cell and maintained the flow of the cells, NaCl solution was flowed in the left microchannel (L1-L2) at a flow rate of 5 µl min^{-1}. Once both microchannels were filled and flow was maintained continuously, we trapped a few cells in the small extended 'beak' of the right microchannel by changing the direction of the flow by the syringe pump. This process was monitored under fluorescence microscope to observe at trapping in the extended microchannel.

C. vulgaris is a spherical microscopic cell with 2~10 µm diameter and has many structural elements similar to plants.[26] Algae cells contain chlorophyll, which is fluorescent under the green fluorescent light, so the algae cells were observed using fluorescence microscopy and shown in Fig. 5A. For trapping, cells were induced and trapped by the contraction/expansion in the microchannel beak by changing the flow direction at R1 and R2 ports. The trapped algae cells were fixed well into the microchannel beak and shown in Fig. 5B (fluorescence) and 5C (optical). Once we have the cells were trapped in the microchannel, the injection of extra alga cells was stopped and the unwanted cells were removed from the microchannel by washing them with sterilized water. The cross flow of NaCl solution from L1 to R2 was started through nanochannel (as schematically shown in Fig 3(iii). The flow rate was maintained with 2 µl min^{-1} flow rate to keep the trapped cells in their place. An algae cell is large in size (more than 10 µm) and the low flow rate of NaCl solution does not move the cell. The osmotic stress in high concentration of NaCl induced the rupture of alga cell walls in solution following a sudden reduction in osmotic pressure. Lysis of the alga cells was thus triggered and the cell material was released. After the cell lysis is completed, the direction of flow was changed and cell materials along with genetic material (DNA, RNA) tend to flow through nanochannel towards the other side of microchannel. Due to the narrow size of nanochannel, some parts of lysed cell materials were separated on basis of their size in front of nanochannel. Finally the desired cell materials flowed along the microchannel via nanochannel and were collected in vials for further analysis.

After lysis of the cell, the flow of NaCl solution was stopped in left microchannel (L1-L2) and cross flow of sterilized water was started from microchannel R2 to L1. The cell organelles started moving towards microchannel (R1-R2), but due to small dimension of the

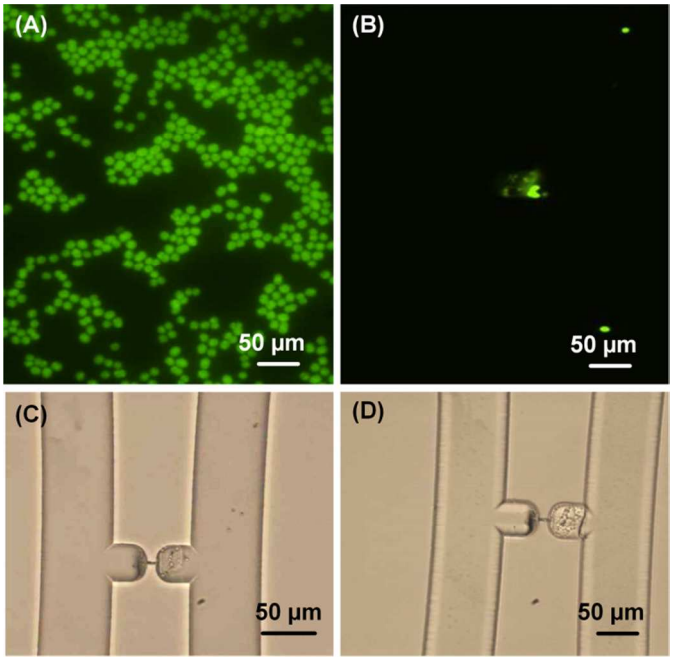

Fig. 5 (A) Fluorescence image of alga cells shows their circular shape and homogeneous distribution (B) trapped alga cells in the side channel (extension made using FIB) before lysis (C) optical image of the trapped alga cells (D) alga cells after the cell lysis.

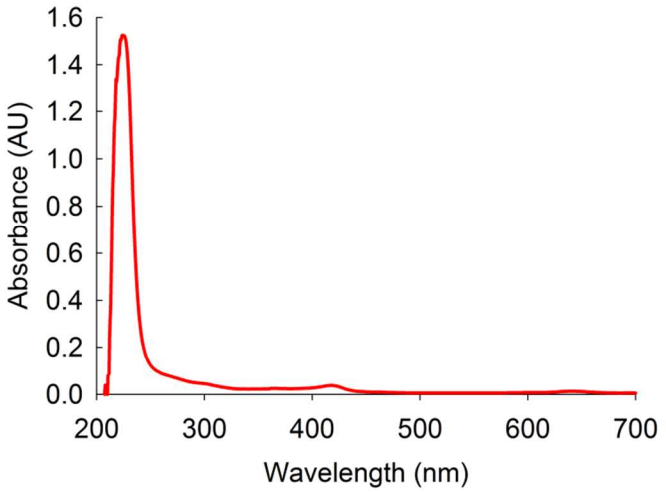

Fig. 6 A wide range UV/IR spectrum for the collected raw material shows the presence of DNA, RNA and other nucleotides peak at range of 230 ~ 290 also trace amount of chlorophyll molecules at 430 nm and 640 nm.

nanochannel only small size molecules can pass through. In this way we separated the small molecules like DNA, RNA and protein along with some cell debris from the rest of the cell materials. The separated molecules are collected and used for further quantification of the material and after filtration through a 0.2 µm filter as discussed in the following section.

Quantitative analysis

Absorbance and fluorescence spectroscopy for quantification of DNA and RNA are powerful tools in life sciences and therefore used for this work for sample analysis. The collected material was first measured and confirmed by UV/VIS spectrometer (Shimadzu UV-visible, UV1601) for quantification of the genetic material. The spectrum was taken on the full range from 200 – 800 nm. A strong peak was observed at the range of 230 – 290 nm, which reports the presence of molecules having double bonds in their chemical structure and are organic in nature (Fig. 6). The DNA, RNA, other protein and nucleotides contain double bonds in their chemical structure. The small peaks at 430 nm and 640 nm were reported about the presence of some chlorophyll molecules, which is present only in trace amounts.

The presence of DNA, RNA and protein in the collected cell material after lysis was quantified by Nano-Drop 1000 as a UV-vis spectrometer. During the measurement, the sample was analysed at 10 mm path length to report information about the available genetic materials.[27] The ratio of absorbance at 260 nm and 280 nm was used to composition of the nucleic acid. If the ratio is appreciably lower than expected, it may indicate the presence of contaminants which absorb at 230 nm. The ratio of absorbance at 260 nm and 280 nm is used to assess the purity of DNA and RNA.[23] A ratio of ~1.8 is generally accepted as "pure" for DNA; a ratio of ~2.0 is generally accepted as "pure" for RNA. If the ratio is appreciably lower in either case in conventional methods, it may indicate the presence of protein, phenol or other contaminants that absorb strongly at or near 280 nm. It is important to note that the actual ratio will depend on the composition of the nucleic acid. If the ratio is appreciably lower than expected, it may indicate the presence of contaminants which absorb at 230 nm. In our study, otherwise, we absorb at 230 nm. In our study, otherwise, we did not worry about contamination to measure absorbance of DNA and RNA using UV/vis spectrometer because no chemicals except NaCl for lysis were used. After sample extraction from the nanofluidic device, an additional off-chip filtration was applied to purify genetic materials. The results of $A_{260/280}$ were 1.84 and 1.97 for RNA and 1.72 and 1.8 for dsDNA before and after filtering, respectively. These ratios are accepted as a pure and the measured data were shown in Table 1. All data are averages from three replicate experiments and the concentration data indicate their standard deviations. After filtering, it was no change for the concentration of DNA. However, the amount of RNA has been lost more than two thirds of the RNA before because it might be degraded. Based on these results, the nanofluidic device shows easy and efficient lysis of cells and extraction of DNA without organic chemicals within short time.

Table 1 Nano-Drop measurements for DNA, RNA and protein molecules in the collected sample, before and after filtration and their ratio $A_{260/280}$.

Type	Conc. (ng/ml)	A_{260}	A_{280}	$A_{260/280}$
Unfiltered				
RNA	3.9±0.6	0.098	0.053	1.84
DNA	3.1±0.3	0.062	0.037	1.72
Protein	38.3±6	-	0.038	-
Filtered				
RNA	1.2±0.2	0.03	0.016	1.97
DNA	2.8±0.6	0.056	0.036	1.8
Protein	11.5±3	-	0.01	-

Conclusions

We have successfully prepared a sealed microfluidic device with nanofluidic channel (100 nm wide, 250 nm deep, and 1µm long) in quartz slide using FIB milling technique combined with wet-etching of microchannels The cross-section of the nanofluidic channel was Gaussian-shaped profile, which was demonstrated to be suitable for extracting cell materials from trapped cells isolated under flow. Cell lysis was carried out using NaCl solution and DNA molecules were extracted from algae cells used as models through the nanofluidic channels under positive pressure. In our experiments, sufficient DNA extraction was achieved to analyze the small sample with a Nano-Drop spectrophotometer. The ratio of $A_{260/280}$ for the extracted material was 1.72 for DNA and 1.84 for RNA, consistent with expectations. These results, confirmed that this type of device with nanofluidic channel enables the separation of very small amounts of bio-samples.[28] Possible outcomes of this study include integration of this kind of nanofluidic channel into a biochip, investigation of the migration of single DNA or protein molecules, or studies of their interactions.

Acknowledgements

The authors acknowledge the financial support of Australian Research Council (FT110100711), and the University of Adelaide. Authors acknowledge support of South Australian Node of the Australian National Fabrication Facility (ANFF), for the start-up award to use their lithography and clean room facility and Australian Microscopy and Microanalysis Research Facility (AMMRF) for use their facilities at Adelaide Microscopy.

Notes and references

[a] School of Chemical and Physical Sciences, Flinders University, Bedford Park Adelaide 5042, Australia.
[b] School of Chemical Engineering, The University of Adelaide, Adelaide, SA5005, Australia.
[c] Ian Wark Research Institute, University of South Australia, Mawson Lakes Adelaide 5095, Australia.
* Prof. Dusan Losic, School of Chemical Engineering, The University of Adelaide, Adelaide, SA5005 Australia, Phone: +61 8 8013 4648,
Email: Dusan.losic@adelaide.edu.au

1 P. Abgrall, and N. T. Nguyen, *Anal. Chem*., 2008, **80,** 2326-2341.
2 H. Andersson, and A. van den Berg, *Curr. Opin. Biotechnol.*, 2004, **15**, 44-49.
3 J. Hong, J. B. Edel, and A. J. deMello, *Drug Discovery Today*, 2009, **14**, 134-146.
4 D. M. Cannon, B. R. Flachsbart, M. A. Shannon, J. V. Sweedler and P. W. Bohn, *Applied Physics Letters*, 2004, **85**, 1241-1243.
5 K. D. Dorfman, S. B. King, D. W. Olson, J. D. P. Thomas, and D. R. Tree, Chemical Reviews, 2012, **113**, 2584-2667.
6 K.-G. Wang, and H. Niu, in *Micro and Nano Technologies in Bioanalysis*, edited by R. S. Foote, and J. W. Lee (Humana Press, 2009), pp. 17.
7 L. D. Menard, and J. M. Ramsey, *Anal. Chem.*, 2012, **85**, 1146-1153.
8 K. Klepárník, and F. Foret, *Analytica Chimica Acta*, 2013, **800**, 12-21.
9 J. O. Tegenfeldt, C. Prinz, H. Cao, R. L. Huang, R. H. Sustin, S. Y. Chou, E. C. Cox, and J. C. Sturn, Anal. Bioanal. Chem., 2004, **378** , 1678-1692.
10 H. Yin, and D. Marshall, *Curr. Opin. Biotech.*, 2012, **23**, 110-119.
11 S. Le Gac, and A. van den Berg, *Trends in Biotechnology*, 2010, **28**, 55-62.
12 A. Ros, W. Hellmich, J. Regtmeier, T. T. Duong, and D. Anselmetti, *Eelectrophoresis*, 2006, **27** , 2651-2658.
13 T. Maleki, S. Mohammadi, and B. Ziaie, *Nanotechnology,* 2009, **20**, 105302-105308.
14 H. Hoang, I. M. Segers-Nolten, J. W. Berenschot, M. J. de Boer, N. R. Tas, J. Haneveld, and M. C. Elwenspoek, *Journal of Micromechanics and Microengineering*, 2009, **19**, 065017-065027.
15 J. W. Hong and S. R. Quake, *Nat. Biotech.*, 2003, **21** , 1179-1183.
16 S. Lindström, and H. Andersson-Svahn, *Biochimica et Biophysica Acta,* 2011, **1810**, 308-316.
17 M. Mahalanabis, J. Do, H. ALMuayad, J. Y. Zhang, and C. M. Klapperich, *Biomedical microdevices*, 2010, **12**, 353-359.
18 M. L. Kovarik and S. C. Jacobson, *Analytical Chemistry*, 2009, **81**, 7133-7140.
19 K. Mawatari, S. Kubota, Y. Xu, C. Priest, R. Sedev, J. Ralston, and T. Kitamori, Analytical Chemistry, 2012, **84**, 10812-10816.
20 L. D. Menard and J. M. Ramsey, *Nano Letters,* 2011, **11**, 512-517.
21 Q. He, S. Chen, Y. Su, Q. Fang, and H. Chen, *Analytica Chimica Acta*, 2008, **628**, 1-8.
22 L. J. Guo, *Advanced Materials*, 2007, **19**,495-513.
23 D. A. Triant and A. Whitehead, Journal of Heredity, 2009, **100**, 246-250.
24 K. Kant and D. Losic, in *FIB Nanostructures*, edited by Z. M. Wang (Springer, 2013), pp. 1-22.
25 J. A. Glasel, *Biotechniques*, 1995, **18**, 62-63
26 C. Safi, B. Zebib, O. Merah, P. Pontalier, C. Vaca-Garcia, *Renewable and Sustainable Energy Reviews*, 2014, **35**, 265-278.
27 P. R Desjardins and D. S. Conklin, *Current Protocols in Molecular Biology* (John Wiley & Sons, Inc., 2011), A. 3J.1-A. 3J.16.
28 R. N. Zare and S. Kim, *Annu. Rev. Biomed. Eng*., 2010, **12** , 187-201.

